J. Fluid Mech. (1987), *vol.* 177, *pp.* 381–394
Printed in Great Britain

An experimental study of strongly nonlinear waves in a rotating system

By DOMINIQUE P. RENOUARD, GABRIEL CHABERT D'HIÈRES AND XUIZHANG ZHANG†

Institut de Mecanique de Grenoble, B.P. 68 F-38402 Saint Martin D'Heres Cedex, France

(Received 30 June 1986)

The influence of rotation upon internal solitary waves is studied in a (10 m × 2 m × 0.6 m) channel located on the large rotating platform at Grenoble University. We observe an intumescence which moves along the right-hand side of the channel with respect to its direction of propagation. Along the side, once the intumescence reaches its equilibrium shape, the height variation of the interface with time is correctly described by the sech^2 function, and the characteristic KdV scaling law linking the maximum amplitude and the wavelength along the side is fulfilled. The intumescence is a stable phenomenon which moves as a whole without deformation apart from the viscous damping. For identical experimental conditions, the amplitude of the intumescence along the side increases with increasing Coriolis parameter, and at a given period of rotation of the platform, the celerity along the side increases with increasing amplitude. But for identical conditions, we found that the celerity along the side is equal to the celerity that the wave would have for such conditions without rotation. The amplitude of the intumescence in a plane perpendicular to the wall decreases exponentially with increasing distance from the side, but the crest of the wave is curved backward.

1. Introduction

The internal solitary waves that are recorded in the oceans have dimensions such that the effect of the Earth's rotation is expected to be non-negligible. But, up to now, there have been few experiments concerning internal solitary waves, and even fewer in rotating systems. Most of the experimental studies are in non-rotating shallow-water conditions (Walker, 1973; Yates 1978; Kao & Pao 1979) and only Koop & Butler (1981) and Kao, Pan & Renouard (1985) provide a large set of comparisons between experimental and theoretical results for a wide range of experimental conditions. But, in rotating system, one can expect some drastic changes such as are suggested, for a nonlinear Kelvin front, by the experimental results of Maxworthy (1983). Analytical results about the effects of rotation on nonlinear waves were obtained by Smith (1972) and more recently by Grimshaw (1985). We present herein some experimental results for solitary internal Kelvin waves. This study should be placed among the work previously done on the large rotating platform at Grenoble University, first devoted to linear internal waves in rotating systems (Chabert d'Hières & Suberville 1976; Kravtchenko & Suberville 1977), and then to nonlinear internal waves but in non-rotating systems (Helal & Molines 1981).

† Permanent affiliation: Institute of Physical Oceanography, Shandong College of Oceanography, P.O. Box 90, Qingdao, China

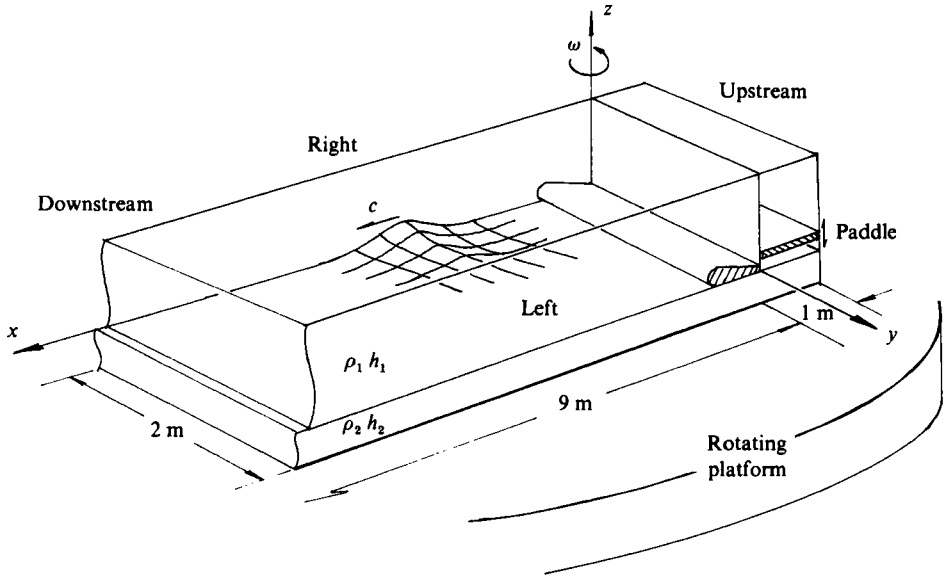

FIGURE 1. The (10 m × 2 m × 0.6 m) channel built on the rotating platform 14 m diameter, and equipped with a paddle.

2. Experimental facility

We used a channel 10 m long, 2 m wide and 0.6 m deep, equipped with a wave generator, which is a horizontal paddle, 2 m wide and 1 m long, moving vertically. The vertical displacements and the time of each of these movements are well controlled and can be accurately reproduced, so that, for a given set of experimental conditions (thicknesses and densities of the upper and lower layers), we can either have several identical displacements of the paddle, or a wide range of displacements, usually of increasing amplitude. For these experiments, the period of platform rotation varied between 50.4 and 150 s, thus covering a wide range variation of the Coriolis parameter f. The interface height variations with time, at a given point, are recorded by an interface follower. This apparatus is a probe electronically directed to follow the movements of a layer of given conductivity with great accuracy. Basically, the principle of this recorder is to measure the conductivity of a given layer, and to compare it with a given reference conductivity chosen by the operator. With this system, we are able to follow the interface with a precision of 0.1 mm in height, and a response time of about 0.5 s. The recordings are made in two ways: (*a*) by analogue recording from a rotary potentiometer, fitted on the same axis as the motor of the interface follower; and (*b*) by a digital optical recorder, fitted on the same axis as the motor, which allows direct data acquisition on a microcomputer. We can use six such interface followers to study the internal phenomena.

3. Experimental results

Along the interface we observe a wave depression if $h_1 < h_2$ and elevation if $h_1 > h_2$. Such a wave, in the absence of rotation, has a horizontal crest perpendicular to the longitudinal axis of the channel and of the sech^2 shape. It propagates at a celerity dependent on the amplitude and given to a first order of approximation by the

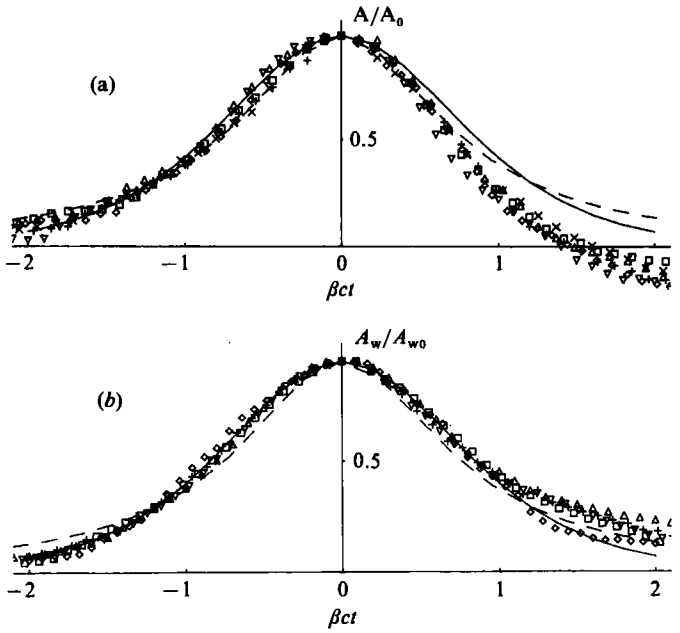

FIGURE 2. Shape of the intumescence along the right-hand wall of the channel: (*a*) without rotation; (*b*) with rotation. The solid line corresponds to the sech² profile, the dashed line to the Lorentzian.

solution of the KdV equation. We can verify that the basic KdV scaling law relating the amplitude to the wavelength is satisfied; namely, that the characteristic wavelength varies inversely as the square root of the wave amplitude (Kao *et al.* 1985).

As soon as rotation is introduced the wave, which is first generated with a horizontal crest, changes its shape in a geostrophic adjustment process. After about ten radii of deformation from the paddle, the intumescence reaches a stable equilibrium shape and then only the viscous damping modifies the intumescence, which is located along the right-hand side of the channel (figure 1). This intumescence propagates in such a way that it is at the right-hand side of the channel with respect to its direction of propagation. The amplitude of the wave decreases with increasing distance from the wall. This wave is followed by a train of dispersive waves, always of much smaller amplitude, and which propagates at a lower celerity.

If we record the shape of this intumescence along the right-hand side, at any point after the wave reaches its equilibrium form we can observe that, whatever may be the experimental conditions (thicknesses and densities of the upper and lower layers) or the rotation speed, the experimental points follow the sech² shape quite nicely (figure 2). But, as pointed out by Koop & Butler (1981), such a test of profile similarity is not very stringent, for we introduce an artificial constraint in requiring that theory and experiment agree at $\beta ct = 0$ and 1.2, where $\beta = [\frac{4}{3}A(h_1 - h_2)/(h_1^2 h_2^2)]^{\frac{1}{2}}$. Since the wave profiles are very similar no large difference between the two waves would be expected. If we record the shape of the wave in various planes parallel to the longitudinal sides, we notice that the experimental points still follow the sech² profile, but increasing scattering develops with increasing distance from the right-hand side (figure 3). This scattering also increases with increasing f.

As one might expect, owing to the geostrophic adjustment in the tank, for identical

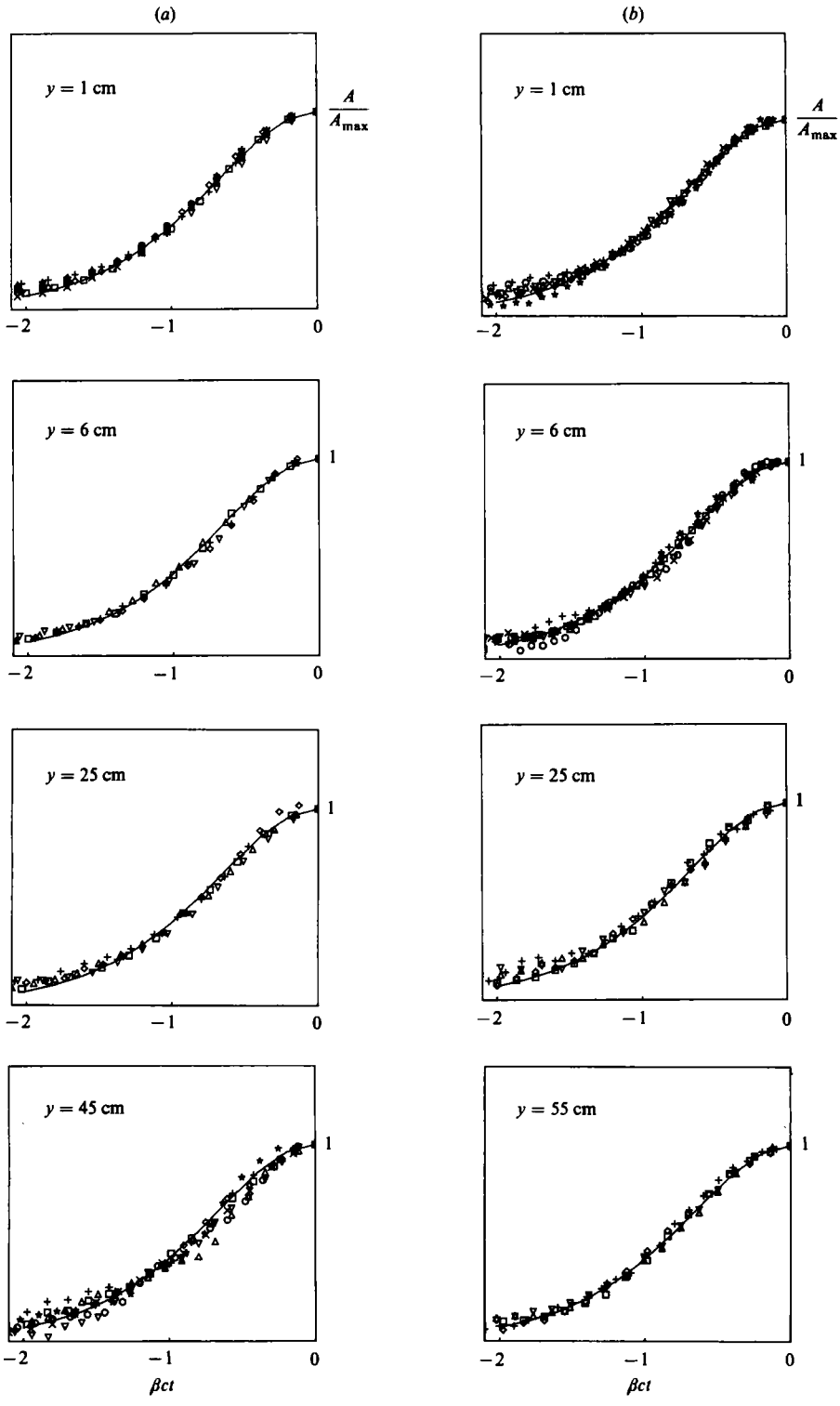

FIGURE 3. Shape of the downstream part of the intumescence in various plans parallel to the right-hand wall for two periods of rotation of the platform: (*a*) $h_1 = 4$ cm; $h_2 = 26$ cm; $\Delta\rho/\rho_2 = 0.012$; $f = 0.249$ s^{-1}; (*b*) $h_1 = 4$ cm; $h_2 = 27$ cm; $\Delta\rho/\rho_2 = 0.013$; $f = 0.0837$ s^{-1}. The solid line corresponds to the sech^2 profile.

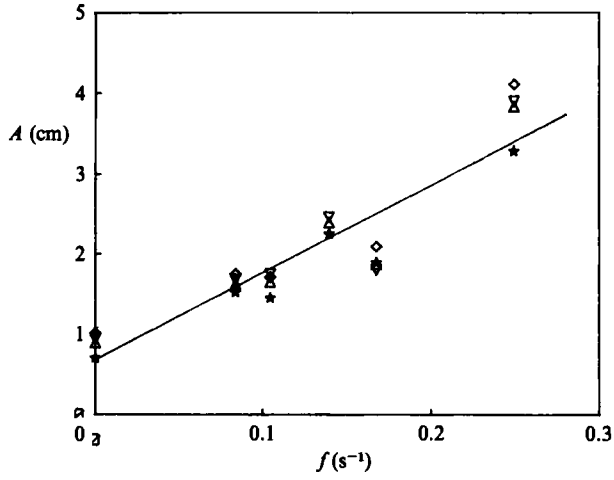

FIGURE 4. Variation with f of the amplitude along the wall at four different locations: ◇, $x = 250$ cm; ▽, 300 cm; △, 350 cm; ★, 400 cm; $h_1 = 4$ cm; $h_2 = 26.5$ cm; $\Delta\rho/\rho_2 = 0.012$.

experimental conditions (thicknesses and densities of the upper and lower layers and displacements of the paddle), the amplitude of the intumescence at a given point along the right-hand side of the tank increases with increasing Coriolis parameter f and it does seem that this increase, at a first order of approximation, is linear (figure 4).

Once the intumescence reaches its equilibrium shape, the amplitude along the wall decreases with increasing distance from the paddle because of viscous damping. The two-layer formulation for the viscous damping of an internal solitary wave in non-rotating axes was first derived by Segur & Hammack (1982) in a manner analogous to Keulegan's (1948) linear formulation of the viscous damping of long surface waves. The equation for the slow decay of an internal solitary wave as it propagates over a long distance is written as

$$\left[\frac{|h_1-h_2|}{h_1 h_2}\eta\right]^{-\frac{1}{4}} - \left[\frac{|h_1-h_2|}{h_1 h_2}\eta_0\right]^{-\frac{1}{4}} = K\frac{\Delta x}{(h_1 h_2)^{\frac{1}{2}}},$$

where

$$K = \frac{\nu^{\frac{1}{2}}}{12(g\Delta\rho/\rho_2)^{\frac{1}{4}}(h_1+h_2)^{\frac{3}{4}}}\left[\left(1+\frac{2h_2}{w}\right)\frac{h_1}{h_2}+\frac{2h_2}{w}+\frac{(h_1+h_2)^2}{2h_1 h_2}\right],$$

and Δx is the distance between the initial observation station, where the stable solitary wave has amplitude η_0, and some other observation station where the amplitude will be η; w is the width of the tank; ν the viscosity, assumed equal in both layers; and g the acceleration due to gravity. This relation has been established without rotation; nonetheless the experiments show that, when the Coriolis parameter is small, there is still a good agreement between the observations and the computations (figure 5*a*, *b*). But when the Coriolis parameter increases, i.e. when the transverse profile becomes significantly different from the horizontal crest, as we shall see below there is only a small deviation from the predicted values (figure 5*c*, *d*), so that there does not seem to be much of an effect of Coriolis forces on viscous damping. One may note that, when the initial observation station taken for this damping computation is too close to the paddle, the agreement between the computed damping

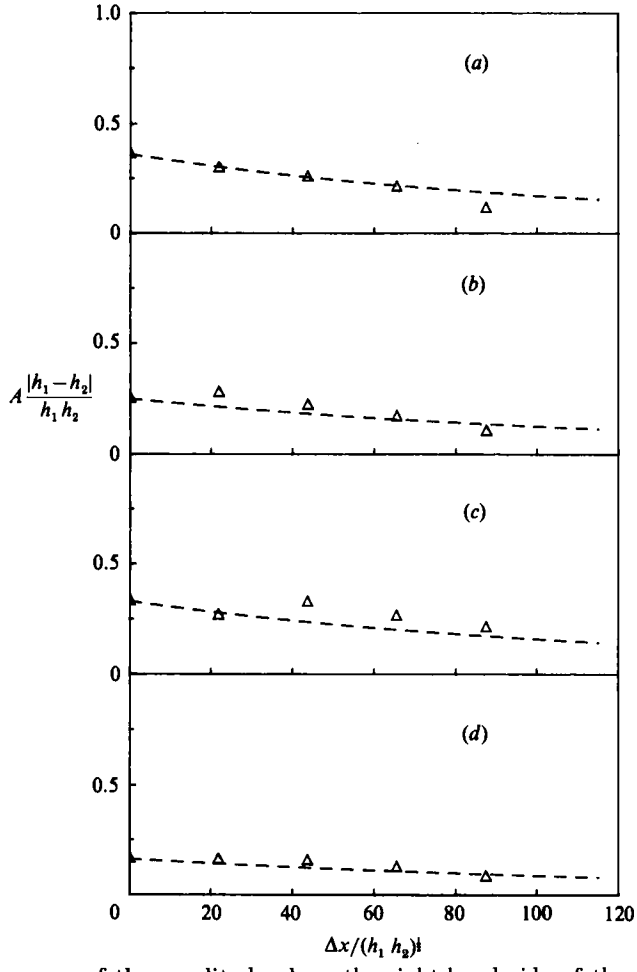

FIGURE 5. Decrease of the amplitude along the right-hand side of the channel due to viscous damping, and comparison with the computed damping (dashed line) for two different paddle displacements. (*a*, *b*) $f = 0.1015\ \text{s}^{-1}$, (*c*, *d*) $f = 0.210\ \text{s}^{-1}$; $h_1 = 1.7$ cm; $h_2 = 12.3$ cm; $\Delta\rho/\rho_2 = 0.017$.

and the experimental data is very poor. The same result was observed for a surface solitary wave (Renouard, Seabra-Santos & Temperville 1985), and is because the formula supposes a stable shape between the two observation stations: such a shape is reached only after some distance from the paddle, in practice for $X > 10R$, where R is the internal radius of deformation.

As already mentioned, as soon as there is rotation, the crest of the wave is neither horizontal nor contained in a vertical plane perpendicular to the side. But it does have a stable shape; that is, if we carefully measure the celerity of this wave along various lines parallel to the wall, we find that after some distance from the paddle, an equilibrium shape is reached, and the wave moves as a whole, without deformation apart from the damping. Once this equilibrium shape is reached, if we consider the profile of a wave in a vertical plane perpendicular to the wall and with its maximum amplitude A_w along the side, we can see that it is exponentially decreasing, $Z = A_w \exp(-Ky)$, with increasing distance from the wall (figure 6*a*). The coefficient of the exponential K is larger than the inverse of the internal radius of deformation.

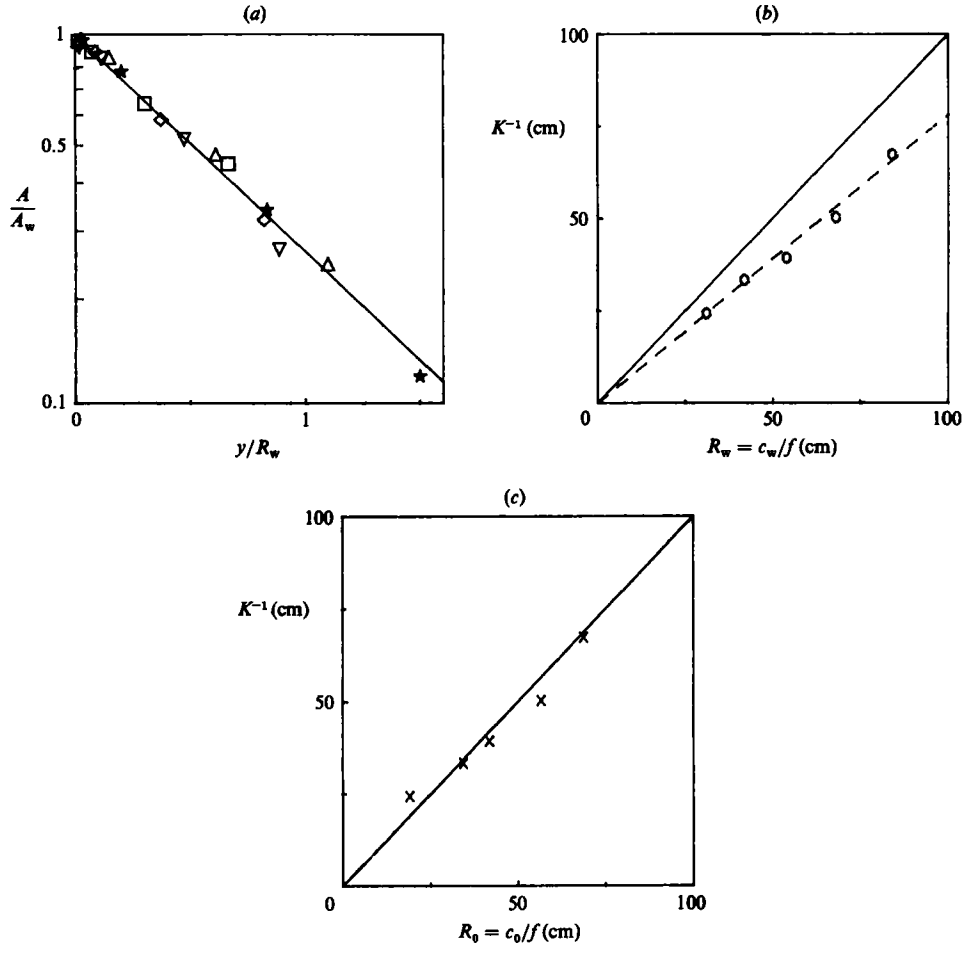

FIGURE 6. (*a*) Amplitude along a line perpendicular to the side. (*b*) Comparison between K^{-1}, a coefficient computed from the data, and R_w, the internal radius of deformation calculated from the actual celerity along the wall. (*c*) Comparison between K^{-1} and R_0, the internal radius of deformation calculated from the linear celerity.

If, to compute this radius of deformation, we use the actual celerity of the wave along the wall, we find that there is a consistent correlation between R and K^{-1}: $K^{-1} = 0.72R_w$ (figure 6*b*). This result is consistent with the data of Maxworthy (1984). Now, if we compute the linear celerity from the actual celerity, i.e. to a first approximation

$$c_0 = c_w\left(1 - \frac{|h_1 - h_2|}{2h_1 h_2} A_w\right).$$

where c_w and A_w are the celerity and amplitude of the wave along the wall, and compare K with $R_0 = c_0/f$, we can see that $K^{-1} = R_0$ (figure 6*c*).

Now, as we said previously, a striking feature of this wave is that the crest of the wave is not contained in a vertical plane perpendicular to side but is curved backward, hence there is a spatial phase shift which increases with increasing distance from the wall, and at a given distance from the wall increases with increasing f (figure 7). If we consider the projection of the crest on a vertical plane perpendicular to the wall

(a)

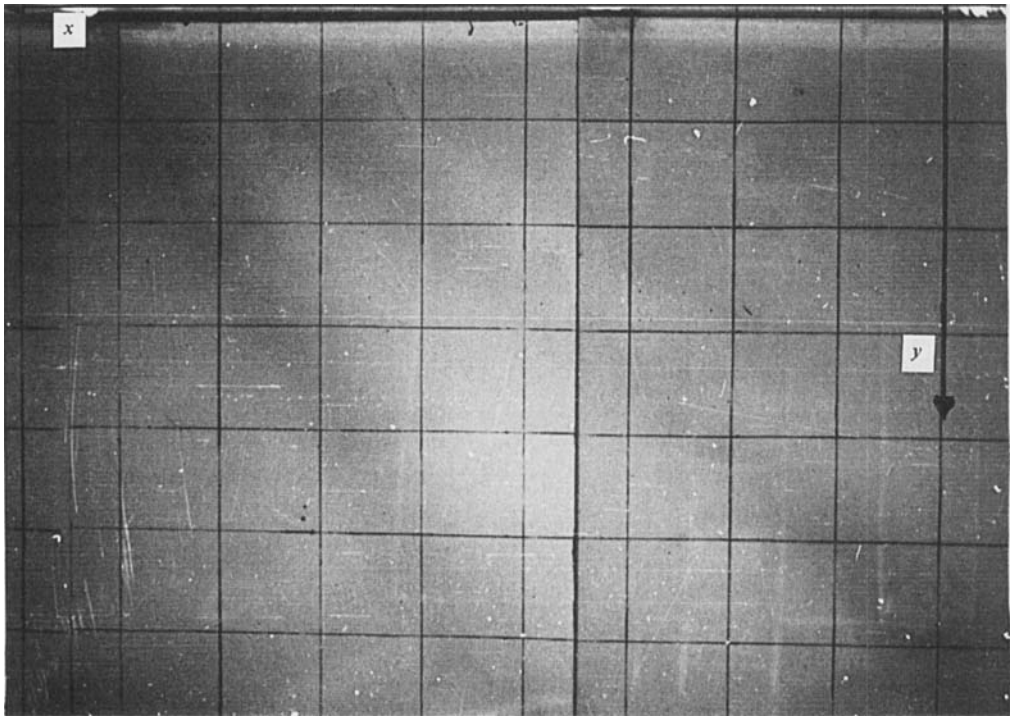

(b)

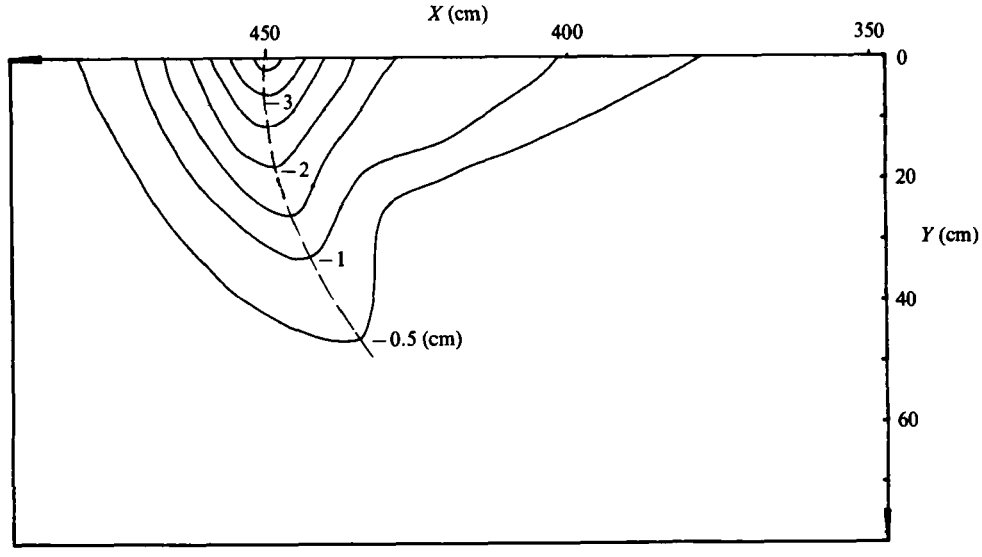

FIGURE 7. (a) Top view of the wave crest, at $x = 4$ m, $h_1 = 1.5$ cm; $h_2 = 12$ cm; $\Delta\rho/\rho_2 = 0.013$; $f = 0.139\ \mathrm{s}^{-1}$. (Owing to a large paddle displacement there are two internal solitary waves). (b) Contour lines of an internal solitary wave; $h_1 = 4$ cm; $h_2 = 26$ cm; $\Delta\rho/\rho_2 = 0.012$; $f = 0.249\ \mathrm{s}^{-1}$.

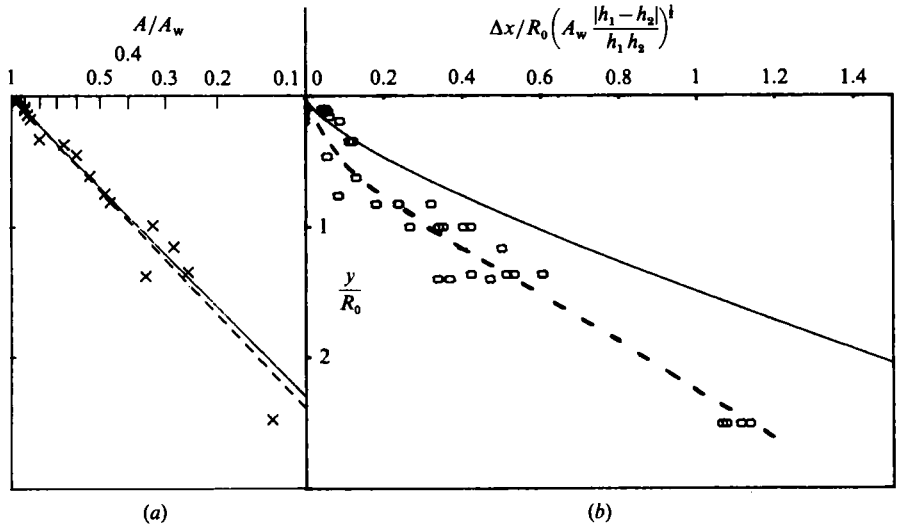

FIGURE 8. (*a*) In semi-log coordinates, a profile of the projection of the crest of the wave upon a vertical plane perpendicular to the side; the dashed line corresponds to $\exp(-K_c y)$, the solid line to $\exp(-y/R_0)$; (*b*) non-dimensionalized spatial phase shift, recorded at various locations and for various periods of rotation of the platform. The solid line corresponds to the approximation deduced from Maxworthy (1983).

and passing through the maximum amplitude of the wave along the wall, we notice that it can be described by $Z = A_w \exp(-K_c, y)$ and, in semi-log coordinates, is slightly above the line $\exp(-y/R)$, as one would expect (figure 8). The relation experimentally found between K_c and R is $K_c^{-1} = 1.04R_0$ ($K_c^{-1} = 1.32R_w$). Since, as noted above, the general shape of the wave is stable, along any line parallel to the wall the spatial phase shift is constant with time once the wave reaches its equilibrium shape. If we non-dimensionalize this spatial phase-shift Δx by the quantity

$$R_0\left(\frac{|h_1-h_2|}{h_1h_2}A_w\right)^{\frac{1}{2}},$$

as suggested by Maxworthy (1983), we see that the experimental observations are along a line which is clearly distinct from the approximation that one can deduce from Maxworthy (1983).

If we now look at the celerities, we can see that, for identical experimental conditions (thicknesses and densities of the upper and lower layers, same rotation period of the platform) and if we increase the paddle displacements and thus the amplitude of the solitary wave, the celerity along the wall will increase roughly following the first approximation given by

$$c_w = c_0\left(1+\frac{|h_1-h_2|}{2h_1h_2}A_w\right)$$

(figure 9). But a new feature revealed by these sets of experiments is that if, for various periods of platform rotation, we carefully keep the same experimental conditions (thicknesses and densities of the upper and lower layers) and the same paddle displacement, we see that the amplitude along the wall increases with f, as previously noted but that the celerity along the wall, measured between the same locations for the whole set of experiments, is constant. Moreover, in a plane parallel to the wall

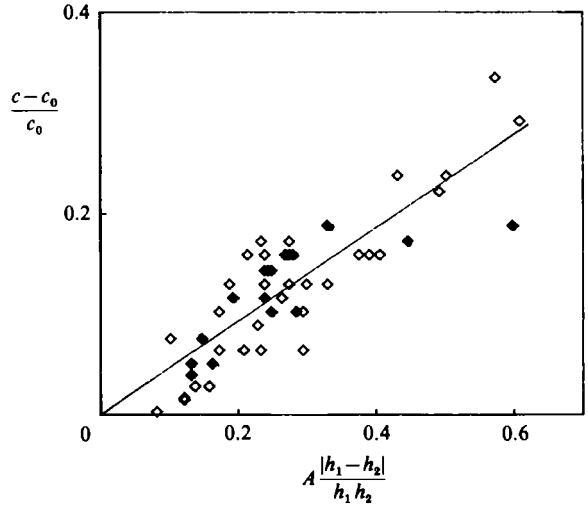

FIGURE 9. Relative increase of celerity along the wall, $(c_w-c_0)/c_0$, versus a reduced amplitude, $|h_1-h_2|/(2h_1h_2)\,A_w$ for two sets of experimental conditions: ◇, $h_1 = 1.7$ cm; $h_2 = 12.3$ cm; $\Delta\rho/\rho_2 = 0.017$; $T_{rot} = 60$ s; ◆, $h_1 = 1.7$ cm; $h_2 = 12.3$ cm; $\Delta\rho/\rho_2 = 0.017$; $T_{rot} = 120$ s.

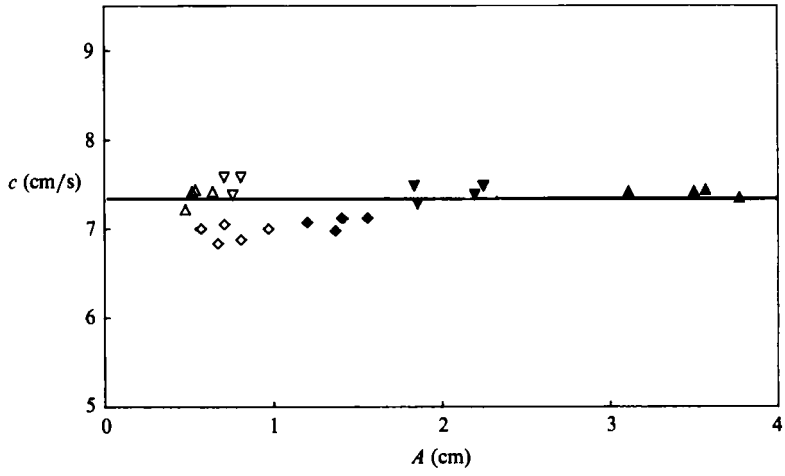

FIGURE 10. Celerity of the wave along the wall (y_0) and at some distance from the wall (y_1) for various periods of rotation, but the same experimental conditions ($h_1 = 4$ cm; $h_2 = 26.5$ cm; $\Delta\rho/\rho_2 = 0.022$). $T_{rot} = 150$ s; ◆, $y_0 = 1$ cm; ◇, $y_1 = 55$ cm; $T_{rot} = 90$ s: ▼, $y_0 = 1$ cm; ▽, $y_1 = 47$ cm; $T_{rot} = 50.4$ s; ▲, $y_0 = 1$ cm, △, $y_1 = 45$ cm. The solid line corresponds to the celerity of solitary waves generated under the same experimental conditions but in the absence of rotation.

and at about one radius of deformation from the wall, the celerity of the wave crest is equal to the celerity along the wall (figure 10). So we get the paradoxical result that a nonlinear wave has a celerity which is constant regardless of the amplitude of the wave. A closer examination of the results shows that this celerity is the celerity of a solitary wave propagating under the same experimental conditions, generated by the same paddle displacement, but without rotation (figure 10). A possible explanation could be that the wave we observe is the end result of a geostrophic adjustment from the horizontal crest intumescence generated by the paddle. Thus,

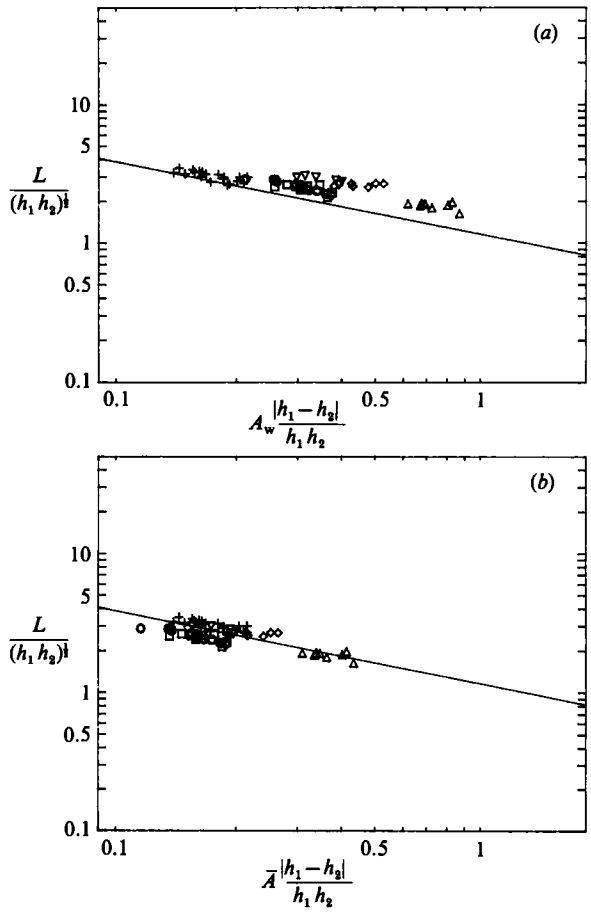

FIGURE 11. (*a*) Relationship between the reduced characteristic length and the amplitude along the wall. The solid line corresponds to the KdV scaling law without rotation (slope $-\frac{1}{2}$). Experimental conditions: $h_1 = 4$ cm; $h_2 = 23$ cm; $\Delta\rho/\rho_2 = 0.012$: +, $f = 0$; ○, $T_{rot} = 150$ s; □, $T_{rot} = 120$ s; ▽, $T_{rot} = 90$ s; ◇, $T_{rot} = 75$ s; △, $T_{rot} = 50.4$ s. (*b*) Relationship between the reduced characteristic length and the average amplitude across the channel. Same experimental conditions as (*a*).

the celerity would be fixed by the amplitude of the horizontal-crest solitary wave first generated by the paddle, itself determined by the volume moved, that is by the paddle displacement, which was constant for this whole set of experiments.

We now turn our attention to the relationship between the reduced amplitude along the wall ($A_w|h_1 - h_2|/h_1 h_2$) and the non-dimensionalized characteristic length-scale, $L_w/(h_1 h_2)^{\frac{1}{2}}$. We first check that the KdV scaling law, which will appear in log–log coordinates as a $-\frac{1}{2}$ slope, is accurately verified in the channel in the absence of rotation. Now, if we introduce rotation, the experimental data, for a given period of rotation, are still along a line of slope $-\frac{1}{2}$, hence the KdV scaling law still holds. But the distance between the lines traced for $f = 0$ and $f \neq 0$ increases with f (figure 11*a*). Though difficult to measure accurately, it seems that, to a first approximation, this distance increases linearly with increasing f. This is consistent with the roughly linear variation of the amplitude with f noted above (i.e. figure 4): the Coriolis effect increases the wall amplitude, hence moving the data to the right in figure 11 (*a*).

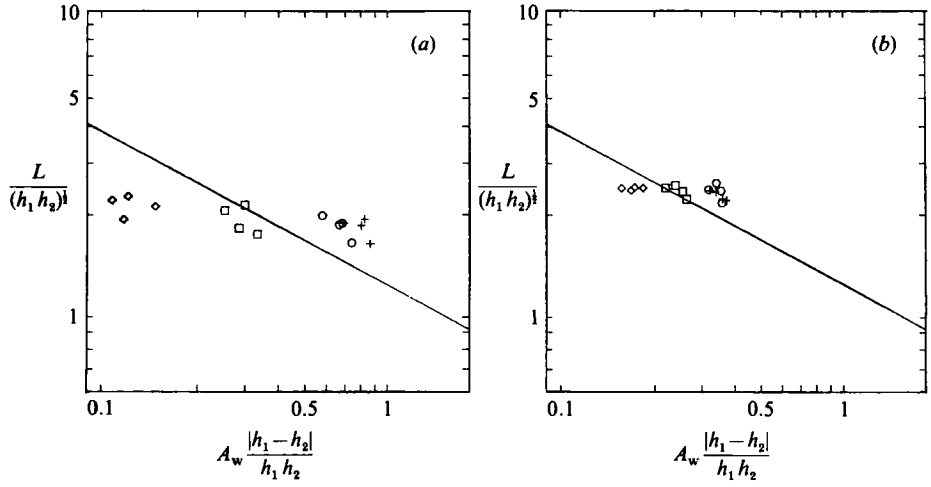

FIGURE 12. Relationship between the reduced characteristic length and amplitude in different planes parallel to the wall. The solid line corresponds to the KdV scaling law without rotation (slope $-\frac{1}{2}$). Experimental conditions: $h_1 = 4$ cm; $h_2 = 23$ cm $\Delta\rho/\rho_2 = 0.012$: □, $y = 1$ cm; △, 6 cm; +, 25 cm; ×, 45 cm or 55 cm; $T_{rot} = 150$ s, 90 s, 50.4 s. (*a*) $f = 0.249$ s^{-1}; (*b*) $f = 0.083$ s^{-1}.

Moreover we checked that if we measure the characteristic length in various planes parallel to the wall, it is almost constant, i.e. independent of y, although the amplitude noticeably decreases (figure 12). If we now use a characteristic wave amplitude across the crest rather than the value at the wall we find a good agreement with the KdV scaling law (figure 11*b*). This characteristic wave amplitude was defined as the amplitude at about one internal radius of deformation from the wall.

Let us note that if, neglecting the crest curvature, we check amplitude of a solitary wave of the same wavelength propagating in a non-rotating channel of finite width L, we find that it is linked with the rotating wave amplitude by the relation:

$$a_{wR} = \frac{A_w[1-\exp(-L/R_0)]}{L/R_0}.$$

Applying this relation for our data, we find that $\bar{a}^*_{wR} = 0.108 \pm 0.027$, the star indicating a non-dimensionalized value, and the bar an averaged value for four different rotation periods of the platform (but same experimental conditions). Granted that it is only an approximation, this is a rather good result which tends to support our hypothesis that both the amplitude, and thus the celerity, and the wavelength are determined by the initial paddle movement, which was identical for all four experiments.

4. Discussion

Thus we have observed a Kelvin-type solitary wave fulfilling the characteristic KdV scaling relationship. The rotation introduces a spatial phase shift so that the wave is curved backward. This wave, once it reaches its equilibrium shape, moves as a whole with a celerity parallel to the wall which is independent of the distance from the wall and equal to the celerity of a solitary wave generated under identical experimental conditions but without rotation.

Using Grimshaw's (1985) classification, our experimental conditions correspond

more closely to the 'strong rotation' case, i.e. internal Rossby radius at most comparable to the wave-length, than to the 'weak rotation' case, i.e. internal Rossby radius much larger than the wavelength, for $0.30 \leqslant L_w/R_0 \leqslant 0.80$ for all experiments. So as noted by Grimshaw (1985) and by Maxworthy (1983), the phase speed and the shape at the channel wall are unaffected by rotation, and we can add that viscous damping is likewise unaffected by rotation. Grimshaw (1985) found that there is a nonlinear influence on the transverse decay scale, but was not able to account for a decay such as Maxworthy's. Since our channel was larger than the internal Rossby radius ($2.4 \leqslant L/R_0 \leqslant 6.7$) only the term associated with the decay scale $K = -f/c_0$ appears, which is in agreement with Grimshaw (1985).

None of the available theory can account for the wave crest curvature, probably because a frictionless fluid is involved. In fact this effect might be due to frictional forces, as one might infer from the work of Brink & Allen (1978) and Mofjeld (1980). Nonetheless we should note that this curvature effect appears whatever the relative thickness of the upper layer is, i.e. whether it is a wave depression (thick lower layer) or a wave surelevation (thin lower layer). So we think that the origin of this curvature is to be found both in higher-order nonlinear effects and in frictional effects. We were unable to measure transverse phase speed, and so can only say that the phase speed measured in planes parallel to the wall was found to be constant, i.e. independent of the distance from the wall, and equal to the celerity that a solitary wave generated in a non-rotating system by the same paddle movement under the same experimental conditions would have. It is also important to note that the front was not curved at the time of generation and that turbulence was only locally observed near the paddle, the wave itself being perfectly smooth, so that the crest curvature cannot be traced to the fact that there was a point-source perturbation. Moreover we think that we have reasonably good experimental evidence that the wave amplitude at the wall is also linked with the amplitude that a wave generated in a non-rotating system by the same paddle movement under the same experimental condition would have. As the same holds true for the wavelength, although with some more scattering, we think that the characteristics of the observed waves are fixed by the paddle movement and the horizontal crest wave it generates, the crest curvature being due to frictional and higher-order nonlinear effects.

We are very grateful to Professor T. Maxworthy for fruitful discussions. And we wish to express our gratitude for MM. R. Carcel, H. Didelle and C. Roche for their help. During this study one of us (X.Z.) was supported by a grant from the Chinese Government. This work was made possible through the financial support of the CNRS (France).

REFERENCES

Brink, K. & Allen, J. 1978 On the effect of bottom friction on barotropic motion over the continental shelf. *J. Phys. Oceanogr.* **8**, 919–922.

Chabert D'Hières, G. & Suberville, J. L. 1976 A theoretical and experimental study of internal waves in a rotating stratified medium. In *Proc. 14th Congress IUTAM, Delft* (ed. W. T. Koiter), vol. 2, pp. 393–405. North Holland.

Grimshaw, R. 1985 Evolution equations for weakly non linear, long internal waves in a rotating fluid. *Stud. Appl. Math.* **73**, 1–33.

Helal, M. & Molines, J. M. 1981 Non-linear internal waves in shallow water: a theoretical and experimental study. *Tellus* **33**, 488–504.

Kao, T. W., Pan, F. S. & Renouard, D. P. 1985 Internal solitons on the pycnocline: generation, propagation, and shoaling and breaking over a slope. *J. Fluid Mech.* **159**, 19–53.

KAO, T. W. & PAO, H. P. 1979 Wave collapse in the thermocline and internal solitary waves. *J. Fluid Mech.* **97**, 115–127.

KEULEGAN, G. H. 1948 Gradual damping of solitary waves. *J. Res. Natl bur. Stand.* **51**, 133–140.

KOOP, G. H. & BUTLER, G. 1981 An investigation of internal solitary waves in a two-fluid system. *J. Fluid Mech.* **112**, 225–251.

KRAVTCHENKO, J. & SUBERVILLE, J. L. 1977 Etude théorique des ondes internes dans les eaux d'un bassin en rotation. *Ann. Hydro.* **5**, 95–115.

MAXWORTHY, T. 1983 Experiment on solitary internal Kelvin waves. *J. Fluid Mech.* **129**, 365–383.

MOFJELD, H. 1980 Effects of vertical viscosity on Kelvin waves. *J. Phys Ocenogr.* **10**, 1039–1050.

RENOUARD, D., SEABRA-SANTOS, F. G. & TEMPERVILLE, A. 1985 Experimental study of the generation, damping and reflexion of a solitary wave. *Dyn. Atmos. Oceans* **9**, 341–358.

SEGUR, H. & HAMMACK, J. L. 1982 Soliton model of long internal waves. *J. Fluid Mech.* **118**, 285–304.

SMITH, R. 1972 Non linear Kelvin and continental-shelf waves. *J. Fluid Mech.* **52**, 379–391.

WALKER, L. R. 1973 Interfacial solitary waves in a two fluid medium. *Phys. Fluids* **16**, 1796.

YATES, C. 1978 An experimental study of internal solitary waves. *AIAA 16th Aerospace Sciences Meeting, Huntsville, Alabama*, Paper No. 78–262.